

1
2
3
4
5
6
7
8
9
10
11
12

SUPPLEMENTAL MATERIALS FOR

Framework humanization optimizes potency of anti-CD72 nanobody CAR-T cells for B-cell malignancies

Temple et al.

Supplemental Methods

Supplemental Figures 1-10

Supplemental Tables 1-3

13 **SUPPLEMENTAL METHODS**

14

15 **Human Cell lines.** Human cell lines were authenticated by short tandem repeat (STR) analysis.

16 Cells were grown in RPMI 1640 medium supplemented with 20% fetal bovine serum (FBS) and
17 100 U/mL penicillin-streptomycin. Cell lines used were routinely tested for Mycoplasma (Lonza,
18 LT07-118) and were negative. SEM, NALM-6, and JeKo-1 cell lines were originally obtained
19 from DSMZ cell bank. Modified cell lines were generated using lentivirus as described in the
20 Method section “CAR-T Cell Production and Expansion.”

21

22 **Molecular Cloning and DNA Plasmids.** Genes encoding the various anti-CD72 nanobody
23 sequences were synthesized as gene fragments from Twist Biosciences (South San Francisco,
24 CA). DNA fragments were then cloned into a lentiviral expression vector with a Gibson
25 assembly product (NEB, E2611S). DNA sequencing was performed to confirm accuracy of the
26 vector. This final construct was then expressed in NEB 5-alpha Competent *E. coli* (High
27 Efficiency) (NEB, C2987H). DNA was isolated using either QIAGEN Plasmid Plus Midi Kit or
28 QiaPrep Spin Miniprep Kit (Qiagen, 27104).

29

30 **Humanization of the Framework Regions in the CD72 Nanobody.** Humanized derivatives of
31 llama NbD4 were generated based on the human variable-heavy chain framework sequence of
32 the clinically approved anti-Her2 antibody Trastuzumab (Herceptin). The thirteen residue
33 positions that varied between llama and human V_H framework were systematically exchanged
34 with their human counterparts in different permutations, resulting in different NbD4 versions
35 (NbD4-H1 through H24) that possess varying degrees of humanization. Llama residues Y37,

36 E44, and R45 in framework region 2 were retained as this region has been shown to be critical
37 for the monomeric nature of nanobodies (marked in green in **Fig. 1A**). Humanized derivatives
38 were then evaluated to resolve the optimal combination that humanizes NbD4 as much as
39 possible, while retaining full CAR signaling efficacy.

40

41 **CAR Engineering.** Empty CAR, CD19, and NbD4 CAR expression plasmids utilized identical
42 components aside from the variable extracellular binding domains (no binder for empty CAR,
43 CD19-directed scFv with clone FMC63, or CD72 directed parental nanobody NbD4). The
44 signaling components including the CD8 hinge and transmembrane domain, 4-1BB co-
45 stimulatory domain, and CD3 ζ signaling domain are identical to those utilized in the clinically
46 approved CD19-directed CAR construct tisagenlecleucel. H24 nanoCAR expression plasmid
47 included the H24 anti-CD72 nanobody binder, an IgG4 hinge region mutated to avoid Fc
48 receptor interaction (“EQ”) (24) a CD28 transmembrane domain, and a CD28 costimulatory
49 domain. All humanized binders, including H1, H2, H3, H4, H5, H6, H7, H8, H9, H10, H11,
50 H12, H13, H14, H15, H20, H23, as well as the affinity matured nanoCAR binders NbD4.1,
51 NbD4.3, NbD4.7, and NbD4.13 all used identical CAR backbones to the H24 nanoCAR
52 construct. Nanobody binders were cloned into the CAR backbone plasmid using Gibson
53 Assembly protocol. CAR expression vectors utilized a green fluorescent protein (GFP) marker
54 for identification of successfully transduced CAR⁺ cells.

55

56 **Lentiviral Vector Production.** Lenti-X 293T cells were transfected with each CAR expression
57 plasmid. Lenti-X 293T cells were cultured for 2-3 days, and then lentivirus was harvested and
58 concentrated using Lenti-X Concentrator (Takara Bio, 631232). Primary human T cells were

59 transduced with lentivirus, and cells underwent spinfection for 120 minutes at 244 RCF to
60 enhance transduction efficiency.

61

62 **CAR-T Cell Production and Expansion.** Primary human T cells were purified from either 1)
63 the leukoreduction filter products of anonymous healthy blood donors from Vitalant (San
64 Francisco, CA) under an institutional review board–exempt protocol in accordance with the U.S.
65 Common Rule (Category 4) or 2) de-identified donor leukapheresis products obtained from
66 StemCell Technologies. CD8⁺ and CD4⁺ T-cell populations were isolated separately using
67 RosetteSep Human T Cell Enrichment Cocktails (Stemcell Technologies, 15023 and 15022) and
68 EasySep Human CD4 T Cell Iso Kit (Stemcell Technologies, 17952) and EasySep Human CD8
69 T Cell Iso Kit (Stemcell Technologies, 17953). CD4 and CD8 cells were thawed, cultured
70 separately in media overnight, and then cells were counted the following day. CD4 and CD8 T
71 cells were mixed in a 1:1 ratio. T cells were cultured in OpTmizer medium with CTS supplement
72 (Thermo Scientific, A1048501) supplemented with 10% human AB serum (HP1022; Valley
73 Medical), and penicillin/streptomycin (Fisher Scientific, 15-140-122) and were passaged every 2
74 days. For expansion, T cells were stimulated with CD3/CD28 Dynabeads (11131-D; Thermo
75 Fisher Scientific) according to the manufacturer’s instructions (20 µL of beads per 1 million T
76 cells) for 5 days and grown in the presence of recombinant interleukin-7 (PeproTech, 200-07)
77 and interleukin-15 (PeproTech, 200-15). Transduction with CAR lentivirus was performed 1 day
78 after the start of bead stimulation. After the removal of CD3/CD28 activation beads, transduction
79 efficiency was assessed by flow cytometry. CAR-T cells were labeled with intracellular GFP, so
80 the percentage of GFP⁺ cells determined the percentage of CAR-T cells generated. All CAR-T
81 constructs included an extracellular Myc tag. To isolate a pure population of CAR-expressing T

82 cells, anti-Myc antibodies (Miltenyi Biotec, 130-124-877) were used for enrichment via MACS
83 column (Miltenyi Biotec, 130-042-401). CAR-T cells were then eluted, cultured in OpTmizer
84 medium with CTS supplement, and expanded for another 4 days. CAR-T cells were cultured in
85 the presence of IL-7 (10 ng/mL) and IL-15 (10 ng/mL), and fresh cytokines were added every 2-
86 3 days. Flow cytometry confirmed similar transduction across all CAR-T cell constructs.

87

88 **Murine Experiments.** All murine experiments were performed under authorization by the
89 UCSF Institutional Animal Care and Use Committee (Approval Number: AN194778-01) and
90 followed all applicable ethical and veterinary guidelines and regulations. NSG (NOD.Cg-
91 *Prkdc^{scid} Il2rg^{tm1Wjl}/SzJ*, Jackson Laboratories) strain mice, bred in-house at the UCSF
92 Laboratory Animal Research Center, were used for all experiments. A mixture of male and
93 female NSG mice, 6 to 10 weeks old, were infused via tail-vein injection with one million B-
94 ALL tumor cells including the SEM cell line, previously modified to stably express luciferase.
95 For JeKo-1 studies, 5e5 effLuc-labeled tumor cells were similarly injected into mice. Tumor
96 burden was quantified via non-invasive bioluminescence imaging (Perkin Elmer In Vivo
97 Imaging System, Caliper Life Sciences) using whole body region of interest gating. Mice were
98 distributed to different experimental arms such that each arm had equal initial tumor burden. One
99 day after distribution, mice received either 1.5e6 or 3e6 CAR-T cells via tail-vein injection. All
100 mouse experiments were conducted with 1:1 CD4:CD8 CAR-T cells. Symptomatic disease was
101 deemed the survival endpoint.

102

103 **Affinity Maturation of anti-CD72 nanobodies based on Nbd4 sequence.** To improve the
104 affinity of nanobody clone Nbd4, we expressed a site-saturation library of Nbd4 variants, fused
105 to the Aga2 protein on the surface of yeast and performed selections for variants with increased
106 affinity for CD72. We generated overlapping oligos that together recapitulated the entire Nbd4
107 sequence, but that incorporate dNTP analogues in every residue position of all three CDR
108 regions while leaving nanobody framework regions unmodified. Assembly of the library using
109 overlap-extension PCR generated a variant library that at most generates one mutation per CDR
110 at a time, resulting in a “soft” mutational variant library. Transformation into the EBY100 yeast
111 strain using electroporation resulted in ~5e8 yeast transformants that were expanded for
112 subsequent yeast display selections. We performed four equilibrium sorts with increasing
113 stringency, starting at a 10nM concentrations of recombinant CD72 protein and ending at
114 100pM, using a combination of MACS and FACS sorting to select higher affinity clones. In
115 order to isolate the highest affinity clones with a low off-rate, we performed two additional
116 selections using 6-hr and 10-hr off-rate sorts with stringent FACS gating on the top 1% of
117 binders. Yeast clones were isolated and sequenced, revealing convergence of key amino acid
118 substitutions including relaxation of I33 residue identity in CDR1 and increased aromaticity in
119 CDR2 represented by either A50W, I51W, or A52F substitutions that together accounted for a
120 significant increase in binding affinity.

121

122 **Expression of CD72 Fc-Fusion and Nanobody Fc-Fusion.** DNA encoding the CD72
123 extracellular domain (amino acids 117–359) was polymerase chain reaction–amplified from a
124 plasmid obtained from the Human ORFeome collection (hORFeome 8.1) and cloned into a
125 mammalian expression vector, fused to the C-terminus of a human constant CH2–CH3 domain

126 (Fc domain), along with a N-terminal Avidity AviTag to facilitate site-specific biotinylation
127 during expression. For expression, 30 µg of plasmid was transiently transfected into Expi293F
128 cells (A14527, modified to stably express ER-localized BirA; Thermo Fisher Scientific) using
129 polyethyleneimine (Transporter 5, 26008-5; Polysciences) at a 4:1 polyethyleneimine:DNA mass
130 ratio. Cells were cultured in Expi293 Expression Medium (A1435101; Thermo Fisher)
131 supplemented with 100 µmol/L biotin for 5 to 7 days to allow for protein expression and
132 biotinylation. To purify recombinant protein, cells were pelleted and the supernatant that
133 contained the protein was recovered, filtered, and pH adjusted with PBS (pH 7.4), prior to
134 loading onto a HiTrap Protein A HP antibody purification column (29048576; Cytiva) to capture
135 the CD72 Fc-fusion protein. The column was washed with PBS, and the protein was eluted with
136 0.1-mol/L acetic acid, then buffer exchanged into PBS using an Amicon Ultra-4 10K device
137 (10,000 MWCO; UFC503008; EMD Millipore). Non-biotinylated nanobody-Fc fusions were
138 similarly purified after expression in unmodified Expi293 cells lacking BirA expression. The
139 concentration of Fc-fusion protein was determined by A₂₈₀ by NanoDrop (Thermo), and
140 molecular weight was confirmed by SDS-PAGE.

141

142 **CAR-T *In Vitro* Cytotoxicity Assays.** Cytotoxicity assays were conducted by mixing target
143 cells with CAR-T cells for 24 hours using the indicated E:T ratios as described in each
144 experiment. For measuring cytotoxicity by bioluminescence with target cell lines stably
145 expressing effLuc, 150 µg/mL of d-luciferin (Gold Biotechnology, LUCK-1G) was added to
146 each sample, incubated for 10 minutes at room temperature, and then read using a GloMax
147 Explorer Plate Reader (Promega). Percent viable cells were normalized to the bioluminescence
148 of tumor cells incubated with untransduced T cells at the corresponding E:T ratios or tumor cells

149 only. Experiments were performed with $n = 3$ to 6 technical replicates. For tumor re-exposure
150 experiments, CAR-T cells were plated with tumor cells stably expressing effLuc at the indicated
151 E:T ratios in each figure. After 24 hours, $1e5$ target cells were added to the remaining CAR-T
152 cells every 24 hours for the indicated number of times in each experiment. Fresh media was
153 added, without IL-7 and IL-15 supplementation, to every tumor rechallenge.

154

155 **Flow Cytometry.** Staining of the cells was performed with either $1e5$ or $5e5$ total cells per
156 sample unless otherwise noted. The manufacturers' recommended amount of antibody was
157 titrated, and an appropriate amount of antibody was used in 100 μ L total volume of fluorescence-
158 activated cell sorting (FACS) buffer (PBS + 5% FBS) for 30 min prior to washing with excess
159 FACS buffer. Samples were immediately analyzed using a CytoFLEX Flow Cytometer
160 (Beckman Coulter). To determine the CAR-T cell memory/stem cell-like characteristics, FlowJo
161 software was used to gate on GFP+ CAR-T cells. The following definitions were used for the
162 various CAR-T immunophenotypes: naïve T cells (CD45RA+/CD62L+), central memory T cells
163 (Tcm: CD45RA-/CD62L+), T-effector memory RA (TEMRA) cells (CD45RA+/CD62L-), and
164 effector memory T cells (Tem: CD45RA-/CD62L-). Antibodies used for flow cytometry are
165 listed in **Supplemental Table 1**.

166

167 **Quantitative Flow Cytometry.** The cell surface quantification of immunotherapy targets CD72
168 and CD19 on tumor cells was used with Quantum™ APC MESF beads (Bangs Laboratories,
169 823). When mice with JeKo-1 tumor were sacrificed, spleens were isolated, crushed, and gently
170 filtered through a 100-micron filter. Red blood cell (RBC) lysis buffer (Fisher Scientific,

171 NC9067514) was used to remove residual RBCs. Residual tumor cells were then washed with
172 FACS buffer (D-PBS + 5% FBS), and antibodies against CD19 and CD72 were added for flow
173 cytometry analysis. Quantum™ APC MESF beads were also included to determine the number
174 of CD19 or CD72 molecules per cell. These beads contain standard numbers of fluorophore
175 molecules per bead to generate a standard curve, and then using the median fluorescence
176 intensity (MFI) and inserting this number into an equation from Bangs Laboratories, the number
177 of CD19 or CD72 molecules per cell was determined.

178

179 **Incucyte Live-Cell Killing Assays.** Healthy donor-derived CAR-T cells were generated against
180 CD72, CD19, or had an empty CAR construct with no antigen binding domain. CAR-T cells
181 were co-cultured against SEM or JeKo-1 cells at the following E:T ratios: 1:1, 1:3, and 1:10. 1e5
182 tumor cells were used in each well, and the number of CAR-T cells varied depending on the E:T
183 ratio in a flat-bottom clear 96-well plate. 200uL of OpTmizer media (same as above) was used
184 per well. Loss of mCherry-positive tumor cells was used to determine cytotoxicity. Data were
185 analyzed using the *Incucyte* Live-Cell Analysis system (Sartorius). Data were normalized using a
186 cytotoxicity index, in which all data were normalized to the initial time point and plotted over
187 time. Co-culture plates were incubated for 4-5 days in the Incucyte, and images were collected
188 every four hours.

189

190 **CAR-T Cytokine Release Assays.** Various CAR-T constructs were cocultured with target cells
191 at a 1:1 E:T ratio, and after 24 hours cells were centrifuged, supernatant was isolated and then
192 snap frozen in liquid nitrogen. Cytokine samples were diluted 1:1 in RPMI + 20% FBS + 1%

193 pen/strep. Eve Technologies used Luminex xMAP technology for multiplexed quantification of
194 14 human cytokines, chemokines, and growth factors. The multiplexing analysis was performed
195 using the Luminex™ 200 system (Luminex, Austin, TX, USA) by Eve Technologies Corp.
196 (Calgary, Alberta). Fourteen markers were simultaneously measured in the samples using Eve
197 Technologies' Human High Sensitivity 14-Plex Discovery Assay® (MilliporeSigma, Burlington,
198 Massachusetts, USA) according to the manufacturer's protocol. The 14-plex consisted of GM-
199 CSF, IFN γ , IL-1 β , IL-2, IL-4, IL-5, IL-6, IL-8, IL-10, IL-12p70, IL-13, IL-17A, IL-23, TNF- α .
200 Assay sensitivities of these markers range from 0.11 – 3.25 pg/mL for the 14-plex. Individual
201 analyte sensitivity values are available in the MilliporeSigma MILLIPLEX® MAP protocol.

202

203 **Bulk RNA-sequencing.** CD8/CD4 CAR-T cells were generated as described above. Bulk RNA
204 was isolated from CAR-T cells before tumor exposure, and after tumor exposure. For CAR-T
205 cells (empty CAR, CD19, and H24) that were exposed to SEM tumor cells, a cytotoxicity assay
206 was set up with a 1:1 E:T ratio. After 24 hours of exposure to SEM, CAR-T cells were isolated
207 with MACS enrichment using anti-cMyc antibodies (Miltenyi Biotec, 130-092-113) to remove
208 any residual SEM cells. The pure CAR-T cell population was centrifuged, and cell pellets were
209 snap frozen in liquid nitrogen. CD8/CD4 CAR-T cells that were not exposed to SEM (pre-tumor
210 CAR-T cells) were included as well for comparison. Triplicate samples for each condition
211 (pretumor vs post-SEM exposure) for each CAR construct (empty CAR, CD19 CAR, and H24
212 CAR) were included. RNA extraction, library preparation, and sequencing were performed at
213 BGI. RNA QC was done with Agilent 2100 Bio analyzer and Agilent RNA 6000 Nano kit.
214 Samples were sequenced using the DNB Seq platform from BGI. For genome mapping, clean

215 reads were mapped to reference genome (hg38) using HISAT. The average mapping ratio to the
216 genome is 95.24% across samples. For gene expression analysis, clean reads were mapped to
217 reference transcripts using Bowtie2 (ver 2.2.5) and expression levels calculated using RSEM
218 (v1.2.8). Gene set enrichment analysis (GSEA) was performed using GSEA software version
219 4.3.0 (Broad Institute).

220

221 **CD19 CAR-T relapsed B-ALL PDX establishment.** A patient derived xenograft sample from a
222 pediatric patient with pre-B ALL was obtained from the pediatric Hematopoietic Tissue Cell
223 Bank (HTCB) at UCSF. The primary peripheral blood sample was injected via the tail vein into
224 an NSG mouse and passaged once. The HTCB study was approved by the Institutional Review
225 Board at the University of California, San Francisco Benioff Children's Hospital and conducted
226 in accordance with the Declaration of Helsinki.

227

228 **Ex vivo cytotoxicity versus PDX-derived tumor.** Patient derived xenograft (PDX) derived from
229 B-ALL patient who relapsed after CD19 CAR-T cells, established from primary tumor collected
230 under an IRB-approved protocol and in accordance with the Declaration of Helsinki. Flow
231 cytometry was used to determine expression of CD19 and CD72. Tumor cells were cocultured
232 with CAR-T cells at indicated E:T ratios for 24 hours in triplicate. Cytotoxicity was measured by
233 staining for CD72-APC expression. Cytotoxicity at each E:T ratio was calculated with the
234 equation:

235 % cytotoxicity = (1 - % APC positive tumor cells / average % APC positive tumor cells cultured
236 with untransduced T cells at the corresponding E:T ratio) x 100%

237

238 **Ex vivo cytotoxicity versus primary B-ALL sample.** Primary adult B-ALL specimens were
239 obtained under an IRB-approved protocol and in accordance with the Declaration of Helsinki.
240 Primary B-ALL bone marrow and peripheral blood samples were assessed for CD19, CD22,
241 CD10, CD34 and CD72 expression. Tumor and CAR-T cells were cocultured for 24 hours at the
242 indicated E:T ratios in triplicate. Cells were stained for CD72 and CD3 to determine cytotoxicity.
243 The values were normalized to untransduced cells incubated with tumor. Cytotoxicity at each
244 E:T ratio was calculated with the equation:

245

246 % cytotoxicity = (1 - % CD3 negative tumor cells / average % CD3 negative tumor cells cultured
247 with untransduced T cells at given effector to tumor ratio) * 100%

248

249 **Biolayer Interferometry.** Bio-layer interferometry data (BLI) was obtained using an Octet
250 RED384 (ForteBio) instrument. Biotinylated CD72 protein was loaded onto a streptavidin
251 biosensor until 0.2-nm signal was achieved. After blocking with 10 uM biotin, each of the
252 nanobody binders was added to determine binding affinity. PBSTB was used a buffer for all
253 analytes. Data were analyzed using the ForteBio Octet analysis software and kinetic parameters
254 determined with a 1:1 monovalent binding model.

255

256 **Retrogenix binder specificity studies.** The Retrogenix Cell Microarray Technology uses
257 HEK293 transiently transfected to overexpress 6,019 secreted and membrane-tethered proteins.
258 Each construct encoding a plasma membrane protein open reading frame also includes zsGreen
259 as a positive control for transfection. Initial binder specificity screens for nanobody test article
260 “H24-Fc fusion” demonstrated consistent binding to CD72-expressing HEK293 cells. Full
261 microarray library screens ($n = 2$) were performed on fixed HEK293 cells with this test article at
262 a concentration of 10 ug/mL. Live cell confirmation screens ($n = 1$) were performed with
263 comparison to rituximab (1 ug/mL) and no antibody as controls for background and false
264 positive hits. Flow cytometry (gated on zsGreen+, live cells) was used to assess binding to final
265 potential hits of CD72 and CBLIF, with CD20 as control. Standard Retrogenix thresholds of
266 fold-change over background are used to assess true- vs. false-positive binding. Retrogenix
267 determined CD72 as the only specific binding partner of H24-Fc fusion, whereas CBLIF binding
268 was determined to be non-significant and consistent with background noise.

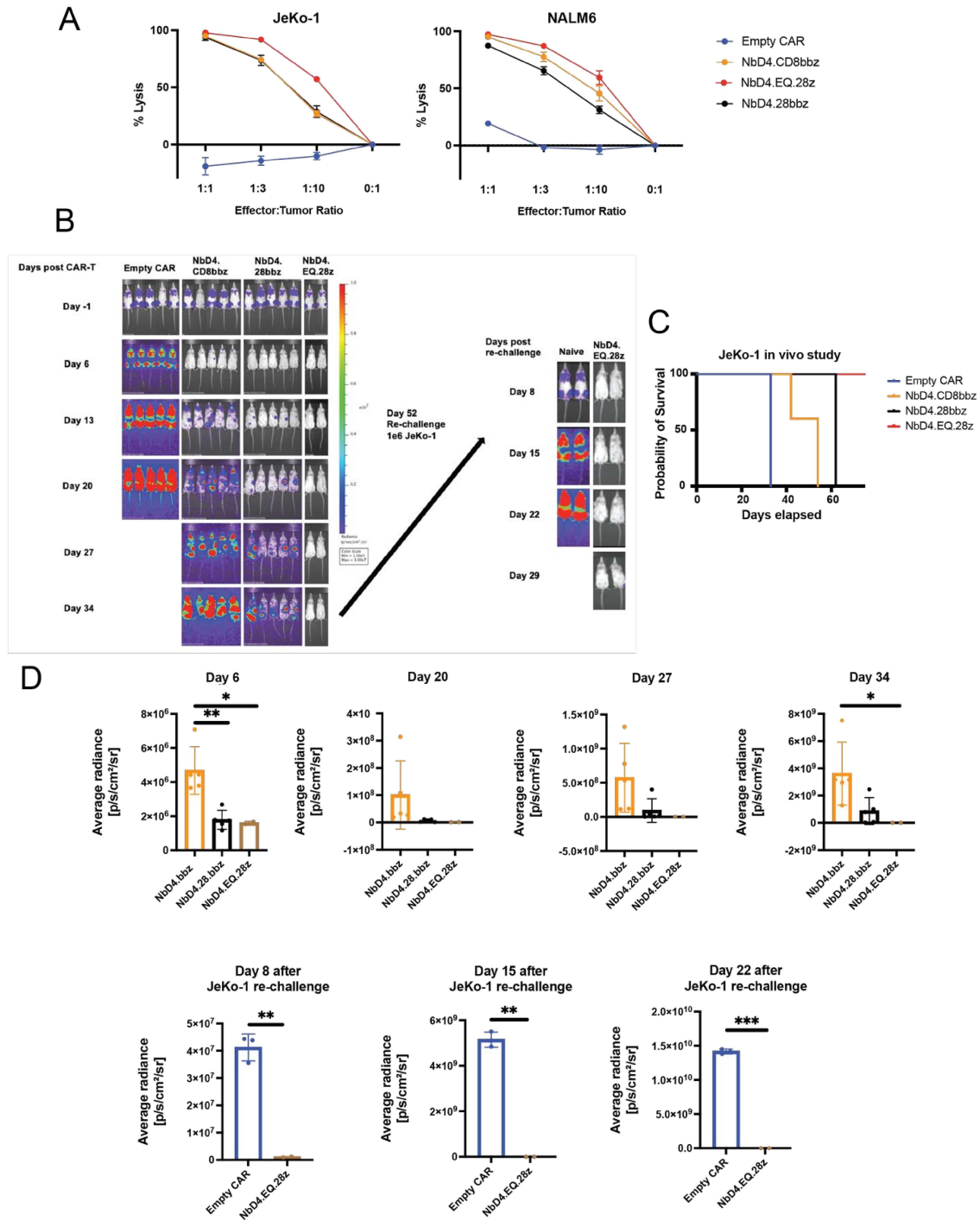
269

270 **Statistical Analysis.** All statistical analyses were performed in GraphPad Prism version 9. Data
271 are presented as mean +/- standard deviation, unless otherwise specified. Statistically significant
272 differences are included in each figure and/or figure legend. All n values given are biological
273 replicates, unless otherwise specified. A $p < 0.05$ was considered statistically significant and p -
274 values were denoted with asterisks as follows ($ns = p > 0.05$, $* = p < 0.05$, $** = p < 0.01$, $*** = p$
275 < 0.001 , $**** = p < 0.0001$). The number of repeats performed, and the statistical tests used, are
276 described in the relevant figure legend.

277

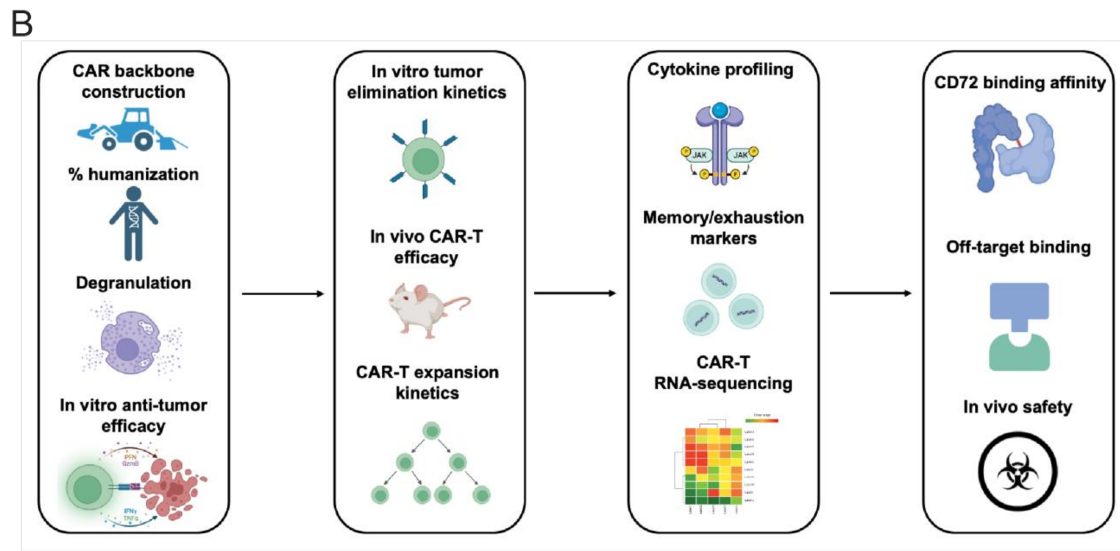
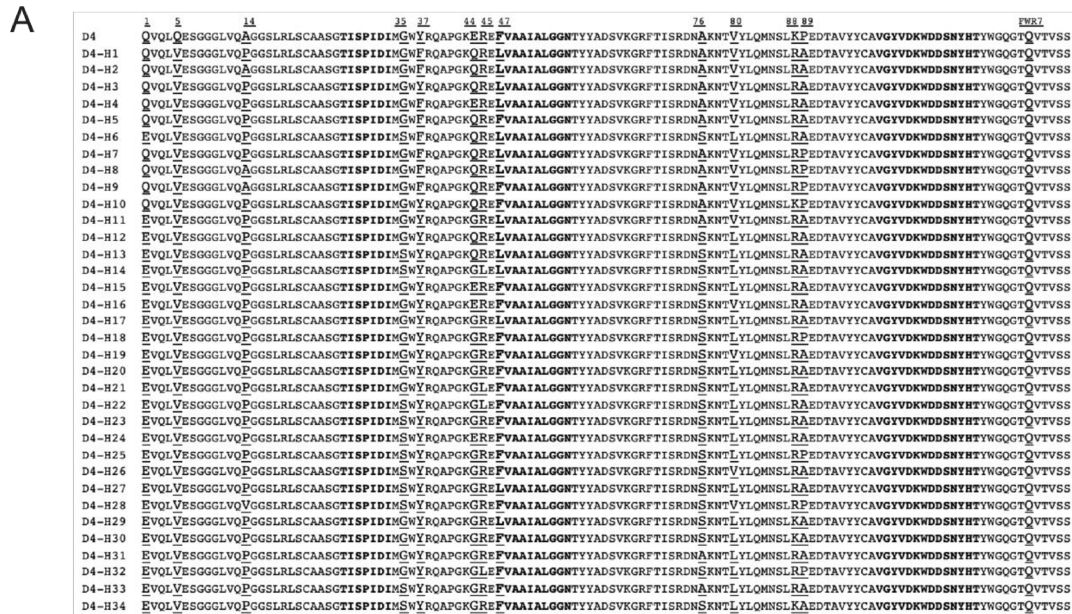
278 **Data availability.** RNA-seq data is publicly deposited to the Gene Expression Omnibus (GEO)
279 repository with accession number: GSE218791.
280
281

SUPPLEMENTAL FIGURE 1



283 **Supplemental Figure 1. NbD4.EQ.28z nanoCARs have potent *in vivo* and *in vitro* anti-**
284 **lymphoma efficacy compared to other CAR backbones. A.** *In vitro* cytotoxicity of NbD4
285 nanoCARs with various CAR backbones were tested against a B-ALL cell line (NALM6) and a
286 mantle cell lymphoma cell line (JeKo-1) at the indicated effector:tumor ratios, cocultured for 24
287 hours. Cell viability was measured via bioluminescence. Data was generated from three
288 biological replicates. Error bars were made using the standard error of the mean, and data were
289 normalized to the tumor only (E:T 0:1) condition. **B.** NSG mice were injected with 1e6 Jeko cells
290 on day -4, and on day 0 mice were treated with 4e6 NbD4 CD72 nanoCARs with the various
291 CAR backbones ($n=5$ mice per arm for Empty CAR, NbD4.CD8bbz, and NbD4.28bbz; $n=2$ mice
292 for NbD4.EQ.28z arm). Due to CAR-T manufacturing challenges with the NbD4.EQ.28z
293 construct for this specific study, there were only sufficient CAR-T cells to include two mice in
294 this treatment arm. BLI was performed on day -1 to randomize the mice into different treatment
295 arms to ensure the disease burden was equal across all CAR constructs. JeKo-1 cells express
296 luciferase, and tumor burden was determined using bioluminescent imaging (BLI). At day 52,
297 mice treated with NbD4.EQ.28z nanoCARs, or naïve mice that were not treated ($n=2$ mice per
298 condition), were re-challenged with 1e6 JeKo-1 cells, and disease burden was followed based on
299 weekly BLI. **C.** Kaplan-Meier survival curves are shown for each of the tested nanoCAR
300 constructs. **D.** Tumor burden was assessed weekly via BLI, quantified BLI images on each day
301 after CAR-T injection are shown. Bar graphs represent the mean \pm S.D. Data in **Supplemental**
302 **Fig. 1C** generated using the long-rank (Mantel-Cox) test. Data in **Supplemental Fig. 1D**
303 generated using an unpaired two-tailed *t*-test. ns = $p > 0.05$, * = $p < 0.05$, ** = $p < 0.01$, *** = p
304 < 0.001
305

SUPPLEMENTAL FIGURE 2



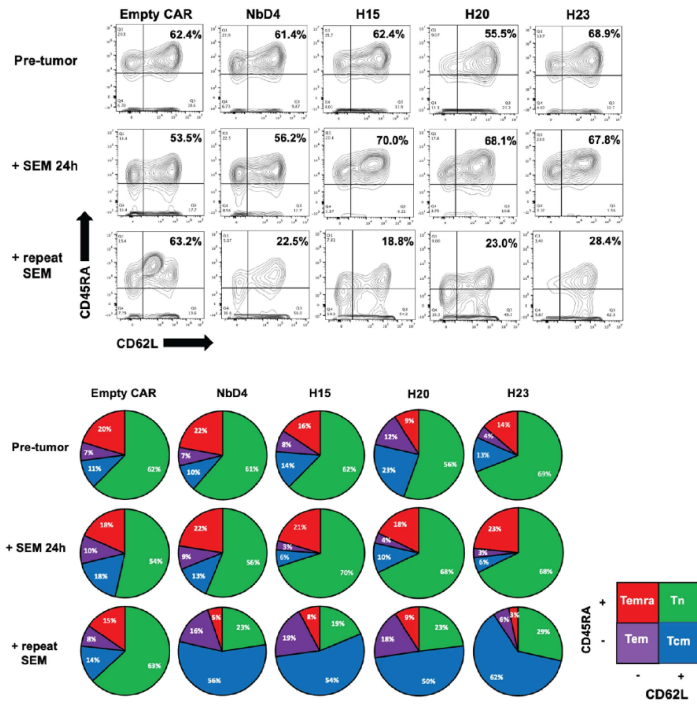
306

307 **Supplemental Figure 2. Framework humanization of Nbd4 and schematic for evaluating**
 308 **humanized nanoCARs.** **A.** Humanization strategy to induce mutations in certain regions of the
 309 framework region in the Nbd4 construct. Amino acid sequence alignments are shown,
 310 comparing parental Nbd4 (D4) to 34 humanized Nbd4 constructs. Amino acid substitutions
 311 were made in the framework regions (specific sites of mutations underlined), while the

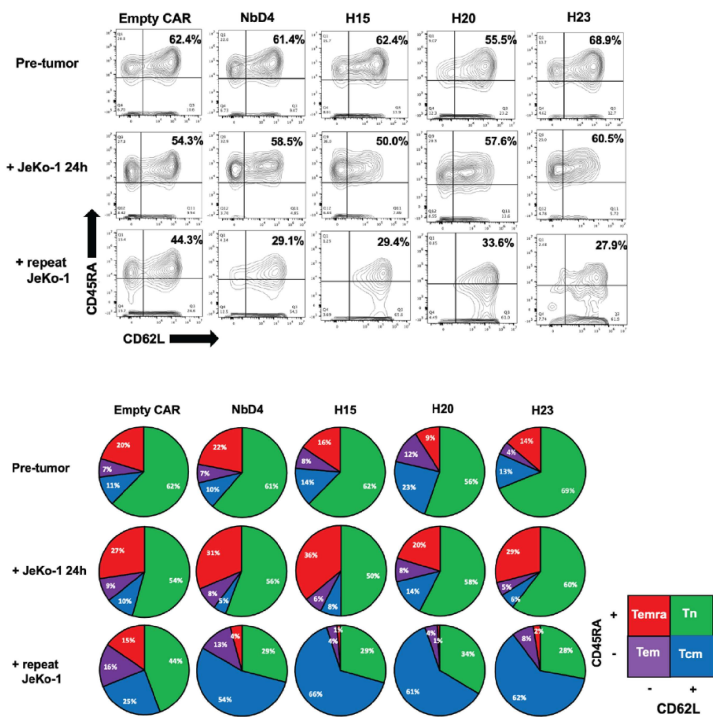
312 complementarity determining regions (CDRs; in bold) were left unchanged. “Human”
313 comparator V_H sequence is derived from the fully human IgG4 monoclonal antibody
314 trastuzumab. **B.** Rationale and characterization of humanized anti-CD72 nanobody CAR-T cells.
315 Figure made with BioRender.
316

SUPPLEMENTAL FIGURE 3

A

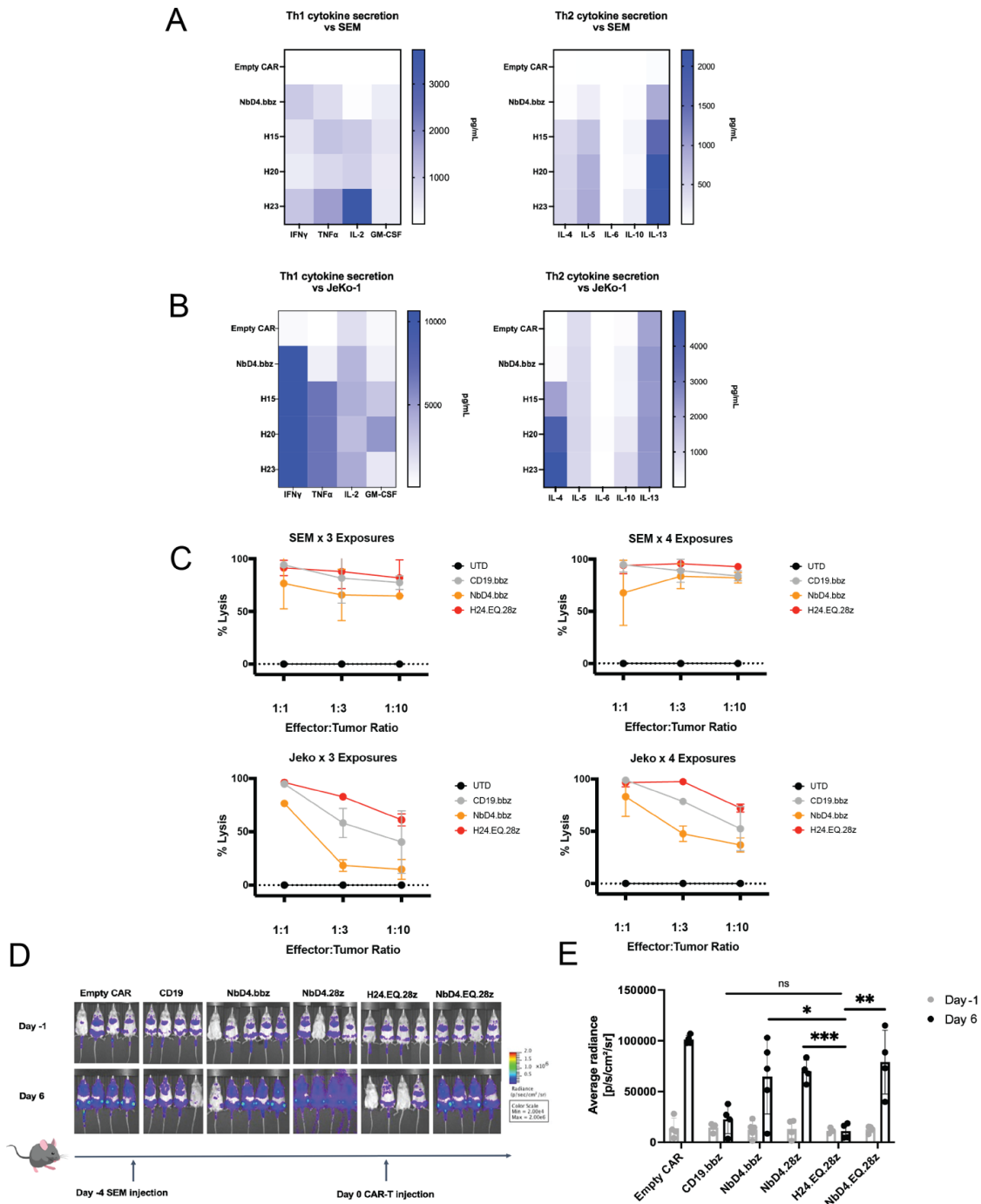


B



318 **Supplemental Figure 3. Memory marker expression on various CD72 nanoCAR constructs**
319 **decreases with repeated tumor exposure to SEM and JeKo-1. A.** Various CD72 nanoCARs
320 and empty CAR-T cells were generated, and flow cytometry was performed to determine cell
321 surface expression of CD45RA and CD62L pre-tumor exposure. Each of the CAR-T cell
322 constructs were then co-cultured with SEM tumors at a 1:1 effector:tumor (E:T) ratio (1e5 SEM
323 cells) for 24 hours, followed by flow cytometry for CD45RA and CD62L. A second exposure
324 with 1e5 SEM tumor cells was added, and 48 hours later flow was performed for CD45RA and
325 CD62L. Circle plots are shown indicating naïve T cells (CD45RA+/CD62L+), central memory T
326 cells (CD45RA-/CD62L+), T effector memory cells re-expressing CD45RA
327 (CD45RA+/CD62L-), and effector memory T cells (CD45RA-/CD62L-). *N* = 1 replicate. **B.**
328 Various CD72 nanoCARs and empty CAR-T cells were generated, and flow cytometry was
329 performed to determine cell surface expression of CD45RA and CD62L pre-tumor exposure.
330 Each of the CAR-T cell constructs were then co-cultured with JeKo-1 tumors at a 1:1
331 effector:tumor (E:T) ratio (1e5 JeKo-1 cells) for 24 hours, and flow cytometry was done for
332 CD45RA and CD62L. A second exposure with 1e5 JeKo-1 tumor cells was added, and 48 hours
333 later flow was done for CD45RA and CD62L. Circle plots are shown indicating naïve T cells
334 (CD45RA+/CD62L+), central memory T cells (CD45RA-/CD62L+), T effector memory cells re-
335 expressing CD45RA (CD45RA+/CD62L-), and effector memory T cells (CD45RA-/CD62L-). *n*
336 = 1 replicate.
337

SUPPLEMENTAL FIGURE 4



338

339 **Supplemental Figure 4. Humanized CD72 nanoCARs have a unique cytokine secretion**
 340 **profile and retain potent anti-tumor efficacy upon multiple tumor exposures. A. CAR-T**

341 cells were co-cultured with SEM tumor cells at a 1:1 E:T ratio for 24 hours. Multiplexed
342 cytokine profiling from culture supernatant after 24-hour SEM exposure. Heatmaps were
343 generated for Th1 or Th2-type cytokine secretion. $n = 1$ replicate. **B.** CAR-T cells were co-
344 cultured with JeKo-1 tumor cells at a 1:1 E:T ratio for 24 hours. Multiplexed cytokine profiling
345 from culture supernatant after 24-hour JeKo-1 exposure. Th1 and Th2 cytokine profiles are
346 shown in the heatmaps. $n = 1$ replicate. **C.** *In vitro* 24-hour cytotoxicity assays comparing H24,
347 NbD4, and CD19 CAR-T cells against SEM or JeKo-1. Every 24 hours, $1e5$ SEM or $1e5$ JeKo-1
348 tumor cells were added to each CAR-T cell construct. The third and fourth SEM or JeKo-1
349 tumor exposures are shown. Data are normalized to untransduced T cells (UTD). $n = 3$ biological
350 replicates. **D.** NSG mice were injected with $1e6$ firefly-luciferase labeled SEM B-ALL cells on
351 day -4, and on day 0 mice were treated with a low-dose *in vivo* CAR stress test with $1.5e6$ CAR-
352 T cells per mouse (1:2 to 1:4 ratio of CD8/CD4 CAR-T cells). BLI was performed on day -1 to
353 randomize the mice into different treatment arms to ensure the disease burden was equal across
354 all CAR constructs. **E.** Tumor burden was assessed on day -1 and day 6 by BLI, and quantified
355 BLI images are shown. The data from all mice are averaged, and error bars represent standard
356 deviation. Data **Fig. 3E** generated using an unpaired two-tailed t-test. ns = $p > 0.05$, * = $p < 0.05$,
357 ** = $p < 0.01$, *** = $p < 0.001$
358

360 **Supplemental Figure 5. H24 nanoCARs have similar in vitro and in vivo proliferation to**
361 **CD19 CAR-T cells. A.** Empty CAR, H24 nanoCARs, and CD19 CAR-T cells were co-cultured
362 with SEM tumor cells at 1:10 E:T ratio for 120 hours; data obtained using Incucyte live-cell
363 imaging ($n = 6$ technical replicates). **B.** Empty CAR, H24 nanoCARs, and CD19 CAR-T cells
364 were co-cultured with JeKo-1 tumor cells at 1:10 E:T ratio for 120 hours; data obtained using
365 Incucyte live-cell imaging ($n = 6$ technical replicates). **C.** NSG mice were injected with $1e6$
366 luciferase-labeled SEM B-ALL cells on day -4, and on day 0 mice were treated with $2.5e6$ CAR-
367 T cells per mouse. $n = 3-6$ mice per arm. Peripheral blood was sampled from mice on day 17 and
368 day 28. CAR-T cells were determined based on dual positivity for GFP+ and CD3. Bar graphs
369 represent the mean \pm S.D. Data in **Supplemental Fig. 9C** were generated using an unpaired
370 two-tailed t -test. ns = $p > 0.05$, * = $p < 0.05$.

371

372

373

374

375

376

377

378

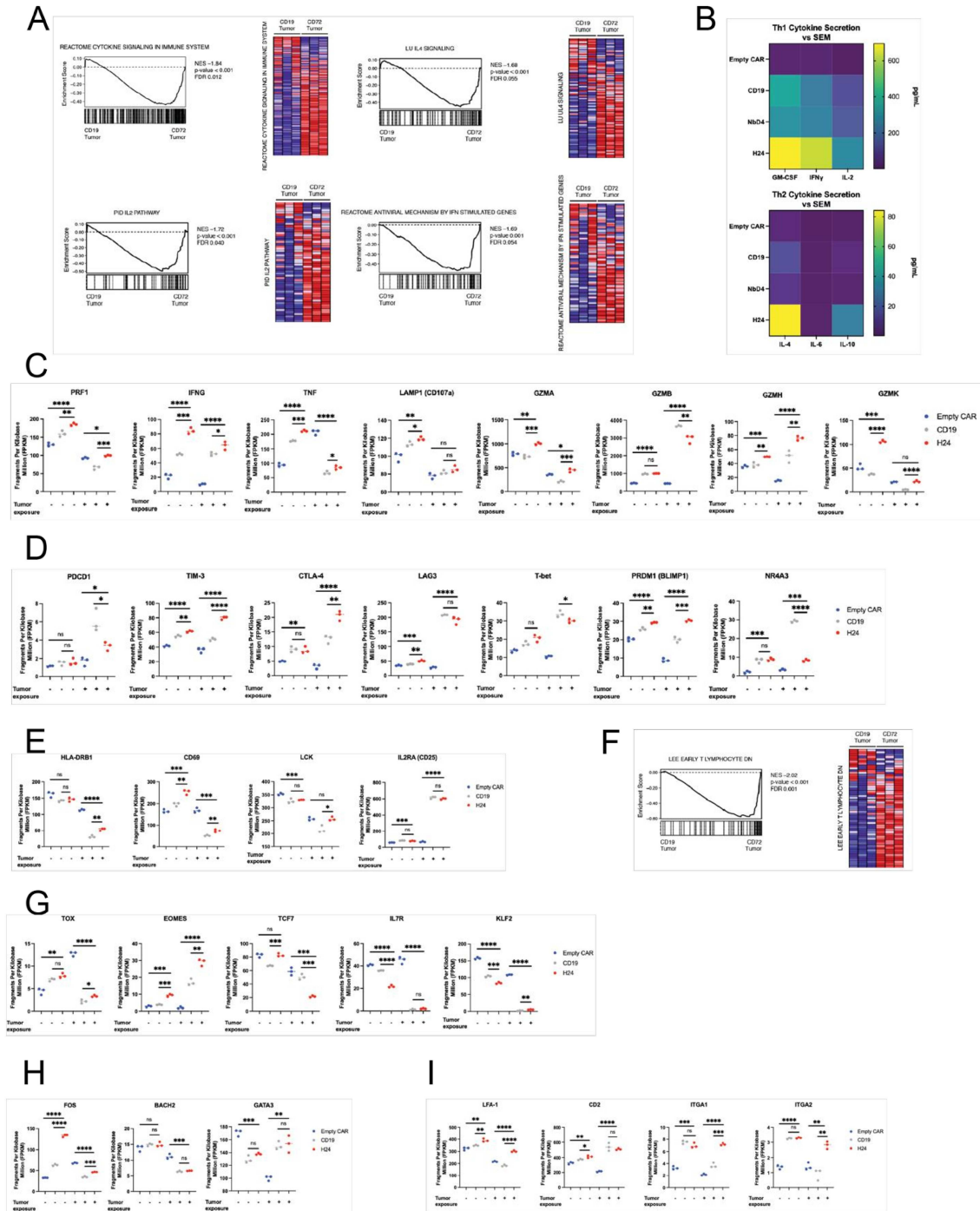
379

380

381

382

SUPPLEMENTAL FIGURE 6



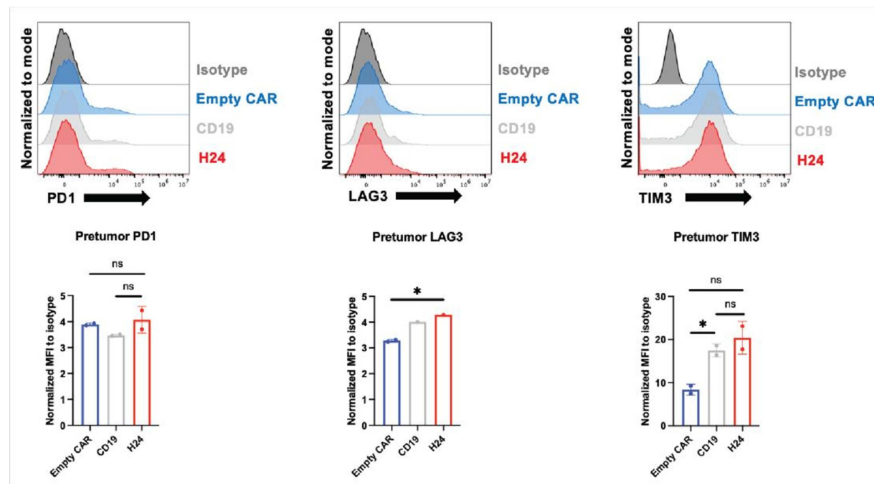
383

384

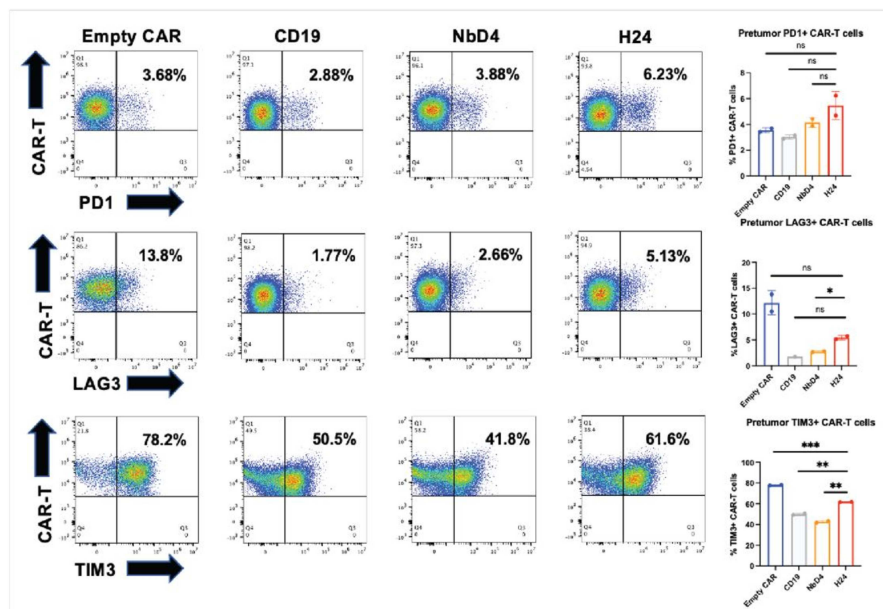
385 **Supplemental Figure 6. RNA-seq reveals that H24 nanoCARs activate unique**
386 **transcriptional pathways, compared to CD19 CAR-T cells, before and after exposure to**
387 **SEM tumors. A.** Gene set enrichment analysis (GSEA) plots and heatmaps showing different
388 transcriptional pathways involved in cytokine signaling that are upregulated in H24 nanoCARs
389 compared to CD19 CAR-T cells, after exposure to SEM for 24 hours. FDR = false discovery
390 rate. **B.** Empty CAR, CD19, NbD4, and H24 CAR-T cells were co-cultured with SEM tumors for
391 24 hours. Multiplexed cytokine profiling from culture supernatant after 24-hour SEM exposure.
392 Heatmaps were generated for Th1 or Th2-type cytokine secretion. Experiment performed in
393 biological triplicate. **C.** Expression of selected cytokines and genes involved in cytotoxicity,
394 before and after exposure to SEM. **D.** Expression of selected inhibitory receptors, before and
395 after exposure to SEM. **E.** Expression of selected genes involved in T cell activation, before and
396 after exposure to SEM. **F.** GSEA plot and heatmap showing a transcriptional pathway involved
397 in early T cell differentiation, after exposure to SEM for 24 hours. **G.** Expression of selected
398 genes involved in stem-like CAR-T cell characteristics, before and after exposure to SEM. **H.**
399 Expression of genes shown to be upregulated in patients with long CAR-T cell persistence
400 greater than six months, before and after exposure to SEM. **I.** Expression of genes important for
401 cell-cell adhesion that are involved in CAR-T elimination of tumor cells, before and after
402 exposure to SEM. Data in **Supplemental Fig. 5C-E; Supplemental Fig. 5G-I** were generated
403 using an unpaired two-tailed t-test. ns = $p > 0.05$, * = $p < 0.05$, ** = $p < 0.01$, *** = $p < 0.001$,
404 **** = $p < 0.0001$
405

SUPPLEMENTAL FIGURE 7

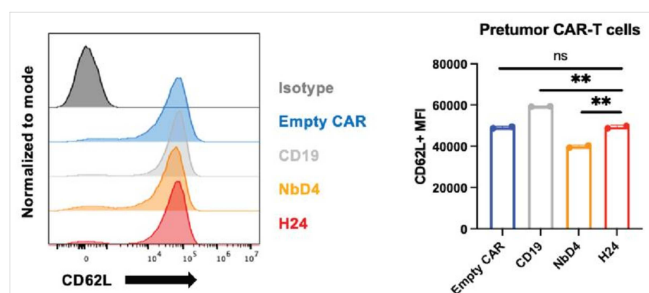
A



B

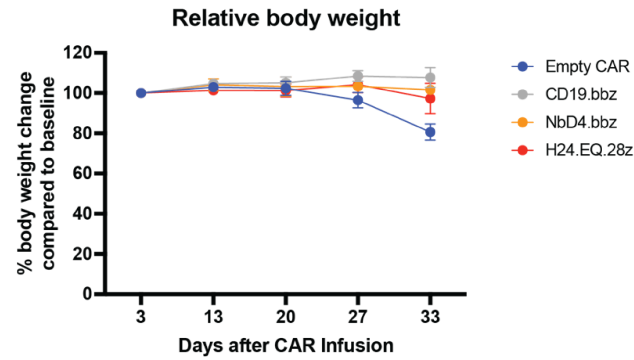


C



407 **Supplemental Figure 7. Pretumor exhaustion marker profiling reveals that H24 nanoCARs**
408 **have similar expression compared to other CAR-T constructs. A.** H24, CD19, and empty
409 CAR-T cells were tested for baseline levels of the exhaustion markers PD1, LAG3, and TIM3 by
410 flow cytometry. The mean fluorescence intensity (MFI) was normalized to each isotype control,
411 and bar graphs are shown for each exhaustion marker. Experiment performed in duplicate. Bar
412 graphs represent the mean +/- S.D. **B.** H24, NbD4, CD19, and empty CAR-T cells were tested
413 for baseline levels of the exhaustion markers PD1, LAG3, and TIM3 by flow cytometry, using a
414 different T cell donor compared to **Supplemental Fig. 6A**. Expression of CAR-T cells that are
415 positive for each exhaustion marker is listed in the upper right quadrant. Experiment performed
416 in duplicate. Bar graphs represent the mean +/- S.D. **C.** H24, NbD4, CD19, and empty CAR-T
417 cells were tested for baseline levels of the memory marker CD62L by flow cytometry. Bar
418 graphs represent the mean +/- S.D. Data in **Supplemental Fig. 6A-C** were generated using an
419 unpaired two-tailed t-test. ns = $p > 0.05$, * = $p < 0.05$, ** = $p < 0.01$, *** = $p < 0.001$
420

421

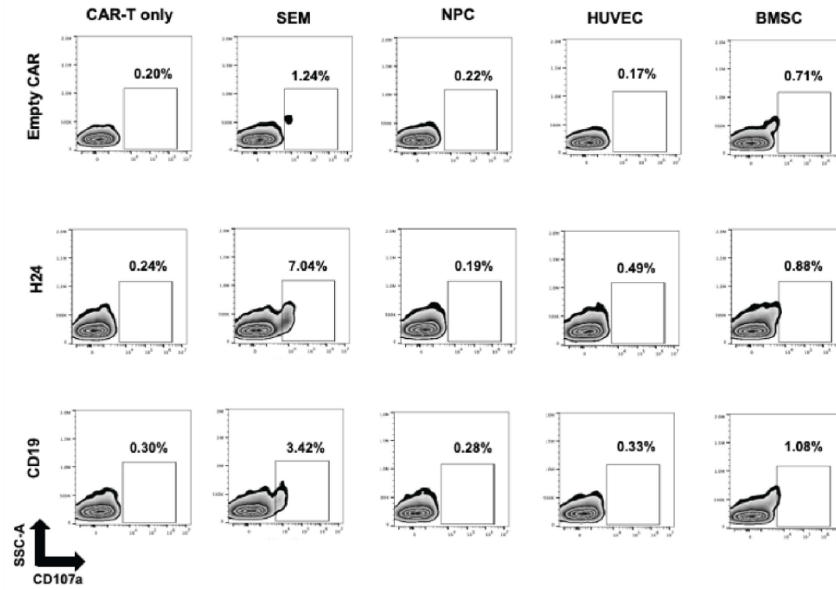
SUPPLEMENTAL FIGURE 8

422

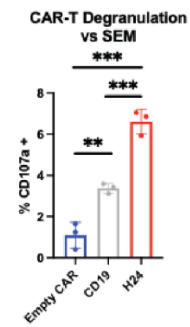
423 **Supplemental Figure 8. Relative mouse body weight over the course of the *in vivo***
424 **lymphoma study in Figure 5.** NSG mice were injected with 5×10^5 firefly-luciferase labeled JeKo-
425 1 mantle cell lymphoma cells on day -4, and on day 0 mice were treated with 3×10^6 CAR-T cells
426 per mouse ($n = 5/\text{arm}$, as shown). During the study, mice weights were obtained once per week.
427 Mouse weights were normalized to the initial weight that was obtained on day 3.

SUPPLEMENTAL FIGURE 9

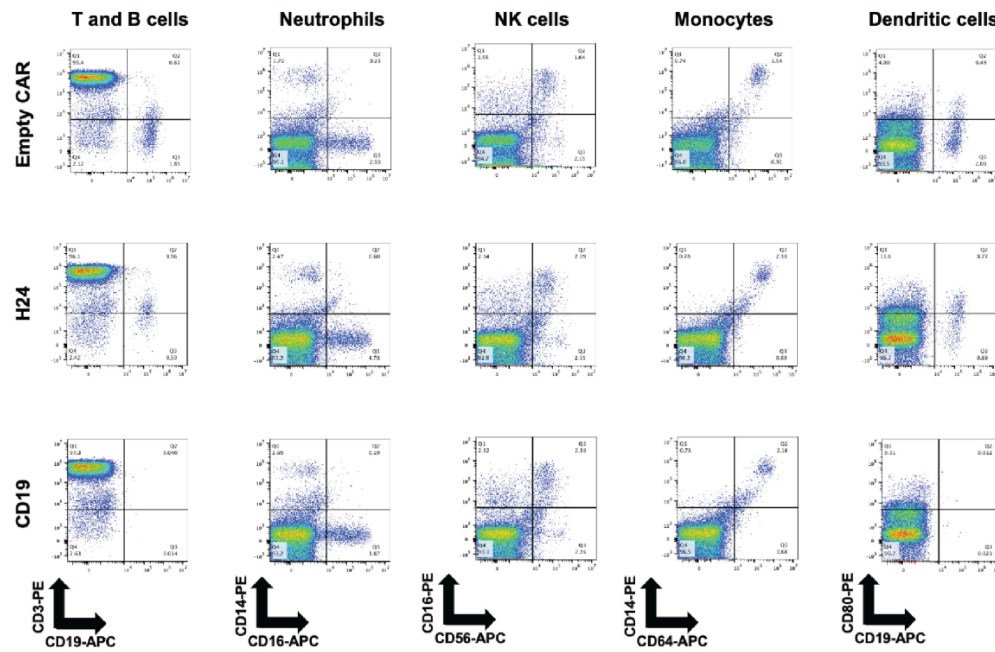
A



B



C



428

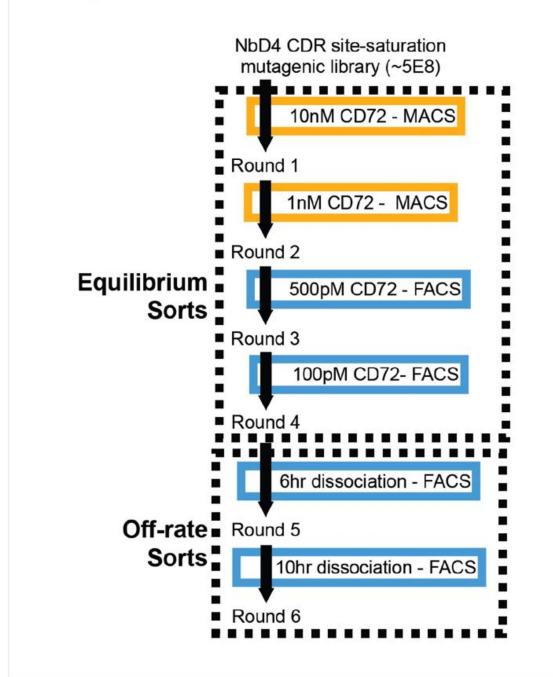
30

429 **Supplemental Figure 9. H24 nanoCARs have a reassuring toxicity profile against normal**
430 **human tissues. A.** *In vitro* flow cytometry-based assay to determine CAR-T degranulation
431 against different target cells using CD107a. H24, CD19, and empty CAR-T cells were generated
432 and co-cultured at a 2:1 E:T ratio against the indicated cell types for six hours. SEM = *KMT2Ar*
433 B-ALL cell line ($n = 3$ technical replicates); NPC = neuronal progenitor cells ($n = 3$ technical
434 replicates); HUVECS = human umbilical vein endothelial cells ($n = 1$); BMSC = bone marrow
435 stromal cells ($n = 1$). Percentage of CAR degranulation is displayed. Bar graph shows CD107a
436 expression against the CD19+/CD72+ SEM cell line. Bar graphs represent the mean +/- S.D. **B.**
437 Flow cytometric analysis of normal donor peripheral blood mononuclear cells (PBMCs) after 24-
438 hour co-culture with either H24, CD19, or empty CAR-T cells. Flow plots display lack of cell
439 ablation for T-cells, neutrophils, NK cells, monocytes, and dendritic cells. B-cells were fully
440 eradicated by CD19 CAR-T cells while partly eradicated by H24 nanoCARs. Experiment
441 performed in duplicate. Data in **Supplemental Fig. 7B** were generated using an unpaired two-
442 tailed t-test. ** = $p < 0.01$, *** = $p < 0.001$
443

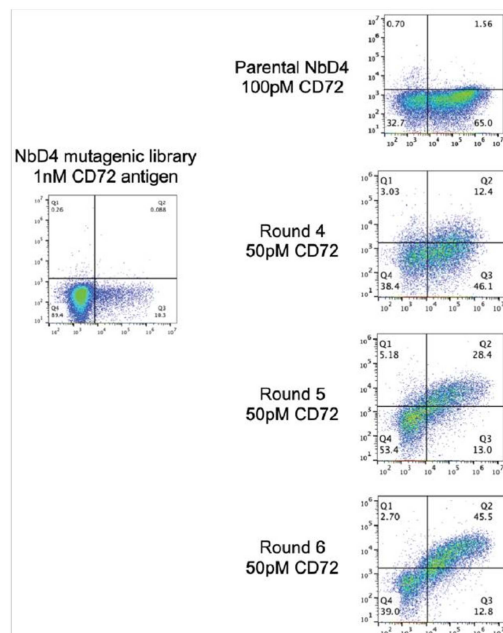
SUPPLEMENTAL FIGURE 10

A

Affinity Maturation Selection Schematic



B



445 **Supplemental Figure 10. Affinity maturation of CD72 nanobody binders. A.** Affinity
446 maturation selection schematic. **B.** Six total rounds of MACS and FACS selections were
447 performed with a CDR site saturated NbD4 yeast display library to isolate variants with
448 increased binding affinity for CD72. Four equilibrium sorts of increasing stringency were
449 performed, followed by two high-stringency kinetic off-rate sorts of 6-hrs and 10-hrs with FACS
450 gating on the top 1% of binding clones. *y*-axis of flow cytometry plots represents FITC-
451 conjugated recombinant CD72 bound to yeast; *x*-axis represents HA staining of yeast
452 successfully expressing a surface nanobody.

453

Antibody, clone	Manufacturer	Catalog number
Human CD72-APC (Clone 3F3)	Biolegend	316210
Human CD19-APC (Clone HIB19)	BD Biosciences	555415
Human CD19-PE (Clone HIB19)	Biolegend	302208
Human CD3-APC (Clone SK7)	Biolegend	344812
Human CD3-PE (Clone UCHT1)	Biolegend	300456
Human CD22-FITC (Clone HIB22)	Biolegend	302504
Human CD34 Pacific Blue (Clone 581)	Biolegend	343512
Human CD10 (Clone HI10a)	Biolegend	312230
Human CD107a-APC (Clone H4A3)	BD Biosciences	560664
Human CD45RA-PE (Clone HI100)	Invitrogen	12-0458-42
Human CD62L-APC (Clone DREG-56)	BD Biosciences	559772
Human PD1-APC (Clone EH12.2H7)	Biolegend	329908
Human LAG3-APC (Clone 3DS223H)	Invitrogen	17-2239-41
Human TIM3-APC (Clone F38-2E2)	Invitrogen	17-3109-42
Alexa Fluor 647 Streptavidin	Biolegend	405237
Human CD16-APC (Clone 3G8)	Biolegend	302011

34

Human CD14-PE (Clone 63D3)	Biolegend	367103
Human CD64-APC (Clone 10.1)	Biolegend	305013
Human CD80-PE (Clone 2D10)	Biolegend	305208

454

455 **Supplemental Table 1. List of all antibodies used for flow cytometry.**

456 B-ALL pediatric patient derived xenograft:

PDX name	Mutation	Treatment status	Cytogenetics	Age	Sex
HM5566	<i>TP53</i> p.R280T, <i>MYC</i> amplification, <i>CDKN2A</i> and <i>CDKN2B</i> deep deletion	Relapse after CD19 CAR-T cells	ETV6-RUNX1 rearrangement	Patient is less than 10 years old	female

457

458

459 B-ALL adult primary patient samples:

Sample name	Mutation	Cytogenetics	Treatment Status	Sex
HMTB0 0911	<i>CDKN2A</i> and <i>CDKN2B</i> loss	45-46,X,- X,add(5)(q11.2),del(5)(q22q33), del(9)(p13),add(11)(q23), ?del(16)(q22)[11]/46,XX[17].nu c ish(ABL1,BCR)x2[173]	Relapse after CD19 CAR- T cells	female
HMTB0 0716	<i>KMT2A</i> r, <i>MYC</i> rearrangement	46XX	Relapse after CD19 CAR- T cells	female

460

461 **Supplemental Table 2.** Patient characteristics of the patient derived xenograft (PDX) and the
462 two primary patient samples that were used in **Fig. 3D-I.**

463

464

SUPPLEMENTAL TABLE 3

Organ System	Empty CAR (H&E)	Empty CAR (IHC for CD3 & CD72)	CD19 (H&E)	CD19 (IHC for CD3 & CD72)	H24 (H&E)	H24 (IHC for CD3 & CD72)
Liver	NSF	NSF	Cellular infiltrate, mononuclear (large cell), rare	Cellular infiltrates negative for CD72 and CD3	Cellular infiltrate, mononuclear (large cell), multifocal, mild	Nodular cellular infiltrate negative for CD3 and CD72
Spleen	Nodular cellular infiltrate (presumed lymphoid, large cell), multifocal, mild to moderate	CD72: Scattered CD72+ cells; CD3: Absence of CD3+ cells. Nodular aggregates negative for CD72 and CD3.	Nodular cellular infiltrate (presumed lymphoid, large cell), multifocal mild	CD72: Scattered CD72+ cells; CD3: Absence of CD3+ cells	Nodular cellular infiltrate (presumed lymphoid, large cell), multifocal, moderate	CD72: Scattered CD72+ cells; CD3: Absence of CD3+ cells
Kidney	NSF	NSF	NSF	NSF	NSF	NSF
Adrenal gland	NSF	NSF	NSF	NSF	NSF	NSF
Pancreas	NSF	NSF	NSF	NSF	NSF	NSF
Lung	Minimal, alveolar histiocytosis	NSF	Minimal, alveolar histiocytosis	NSF	Minimal, alveolar histiocytosis	NSF
Heart	NSF	NSF	NSF	NSF	Endocardiosis, mild	NSF
Stomach	NSF	n/a	NSF	n/a	NSF	n/a
Small Intestine	NSF	n/a	NSF	n/a	NSF	n/a
Large Intestine	Mural hematoma; protozoa	n/a	Protozoa	n/a	Protozoa	n/a
Brain	NSF	NSF	NSF	NSF	NSF	NSF
Reproductive tract	NSF	n/a	NSF	n/a	NSF	n/a
Lower urinary tract	NSF	n/a	NSF	n/a	NSF	n/a
Skin	NSF	n/a	NSF	n/a	NSF	n/a

465

466 **Supplemental Table 3. Summary autopsy and immunohistochemistry (IHC) evaluation for**
467 **mice who received H24 nanoCARs, CD19 CAR-T cells, or empty CAR-T cells.** NSG mice
468 were injected with 1e6 luciferase-labeled SEM B-ALL cells on day -4, and on day 0 mice were
469 treated with 3e6 CAR-T cells per mouse. $n = 2$ mice per arm. On day 14, mice were sacrificed
470 and H&E staining was done on all major organs was performed as part of a full murine autopsy.
471 Immunohistochemistry against human CD3 was used to determine CAR-T infiltration in murine
472 tissues, and CD72 to determine the presence of SEM tumor cells in different murine tissues. The
473 table represents H&E and IHC results from the study, stratified by each organ system. Summary
474 histopathologic findings from the two mice from each CAR-T treatment arm are reported in the
475 table. A murine pathologist was blinded to the study design and determined that the following
476 histopathologic features were incidental findings: the presence of protozoa in the intestinal tract
477 (cecum), minimal alveolar histiocytosis, intestinal mural hematoma, focal renal tubule dilation,
478 and a single instance of mild endocardiosis. $n = 2$ mice for each CAR treatment arm. NSF = no
479 significant findings. N/A = not available.

38